BIAXIAL TESTING OF FIBRE REINFORCED COMPOSITES

D. Van Hemelrijck[1], C. Ramault[1], A. Makris[1], , A. Clarke[2], C. Williamson[2], M. Gower[3], R. Shaw[3], R. Mera[3], E. Lamkanfi[4], W. Van Paepegem[4]
[1]Vrije Universiteit Brussel, Mechanics of Materials & Constructions, Brussels, Belgium
[2]QinetiQ, Cody Technology Park, Ively Road, Farnborough Hampshire GU 14 OLX - UK
[3]National Physical Laboratory, Hampton Road Teddington Middlesex TW 11 OLW, UK
[4]Ghent University, Laboratory Soete, Mechanical Construction & Production, Ghent, Belgium

Keywords: *biaxial testing, digital image correlation, inverse methods*

Abstract

To study the behaviour of fibre reinforced composite laminates under in-plane complex stress states a biaxial loading frame has been developed. Using four independent servo-hydraulic actuators a cruciform type specimen is biaxially loaded in its plane. For obtaining reliable biaxial failure data the design of the cruciform specimen is of paramount importance. Finite element simulations of the cruciform specimen in combination with experiments using DIC for strain determination has led to the proposal of an optimized geometry which was used to obtain strength data at different loading ratio's. For the identification of the in-plane orthotropic elastic constants an inverse method is presented. The full field displacements and strains are identified by digital image correlation technique and compared with finite element strain results. The engineering constants are unknown parameters in the finite element model. Starting from initial values, these parameters are updated till the computed strain field matches the experimental strain field.

1 Introduction

Although the use of composite materials in aerospace, aviation and automotive industry has increased rapidly over the last decades, reliable rules for the prediction of structural behavior are generally not available and consequently excessive safety factor are used to cover the high level of uncertainty. The ability to successfully model and simulate the behavior of these materials for optimum use in structural applications, depends largely on the material description (constitutive relations, damage evolution laws, failure criteria, ..) employed in the analytical/numerical formulations. For validation of proposed material models rigorous experimental characterization under a variety of complex loading conditions is mandatory. The current practice of using solely uniaxial test results is simply inadequate. In general, composite laminates are developing multi-axial stress states [1] and consequently testing closer to reality is needed. Even though large demand exists for experimental multiaxial test data, there is little existing experimental capability to evaluate the multiaxial response of composite materials [2,3,4]. One of the major difficulties on performing these multiaxial tests is to design specimens and loading devices so that a uniform plane stress state can be produced.

2 Biaxial testing equipment

Different experimental techniques and specimens have been used to produce biaxial stress states. These techniques may be classified into two categories [5], (i) tests using a single loading system and (ii) tests using two or more independent loading systems. In the first category the biaxial stress ratio depends on specimen's geometry or on the loading fixture configuration, whereas in the second category it is specified by the applied load magnitude.

Examples of the first category include bending tests on cantilever beams, anticlastic bending tests of rhomboidal or rectangular shaped composite plates, bulge tests, equibiaxial loading of disc- shaped specimens and tests on cruciform specimens with a spatial pantograph.

Examples of the second category are round bars under bending-torsion, thin-wall tubes subjected to a combination of axial loading and torsion or internal / external pressure, and cruciform specimens under in-plane biaxial loading.
The technique with the thin-wall tube is the most popular one [6] and seems to be very versatile, because it allows tests with any constant load ratio to be performed. However, it presents some inconveniences [5,7,8] as for instance (i) depending on the thickness of the tube and the applied load the radial stress gradients may not be negligible, (ii) real construction components in fibre reinforced composite materials are often flat or gently curved and differ a lot from tubular specimens, (iii) thin-wall tubes are not easy to fabricate, (iv) obtaining a perfect alignment and load introduction is not straightforward, (v) thin tubular specimens can experience various forms of elastic instability when they are subjected to circumferential or axial compression or torsion loads, and (vi) tubes may exhibit changes in geometry during loading, but these effects are usually ignored when processing experimental results. There for the most appropriate method for biaxial testing of fibre reinforced composite laminates consists of applying in-plane biaxial loads to cruciform specimens. In order to do so, a biaxial test device was developed at the Free University of Brussels (VUB) at the Department of Mechanics of Materials and Constructions (MeMC) [9]. This device employs four servo-hydraulic actuators for testing cruciform specimens under static and cyclic loading conditions. Finite element simulations of the cruciform specimen geometry in combination with experiments using both strain gages and a full field optical-numerical method for the strain measurements in the biaxially loaded test zone have been carried out, leading to the proposal of an optimized geometry.

3. Plane biaxial test bench for crucifom test specimens

The biaxial test rig, see Figure 1, developed at VUB has a capacity of 100kN in each perpendicular direction, but only in tension, limiting the experimental results to the first quadrant of the two-dimensional stress space. As no cylinders with hydrostatic bearing used, failure or slip in one arm of the specimen will result in sudden radial forces which could seriously damage the servo-hydraulic cylinders and load cells. To prevent this, hinges were used to connect the specimen to the load cells and the servo-hydraulic cylinders to the test frame. Using four hinges in each loading direction results in an unstable situation in compression and consequently only tension loads can be applied. The stroke of the cylinders is 150mm. The loading may be static or dynamic up to a frequency of 20Hz. Each cylinder is independently controlled and any type of loading waveform, including spectral sequences of variable amplitude, can be efficiently introduced using the dedicated software and control system.

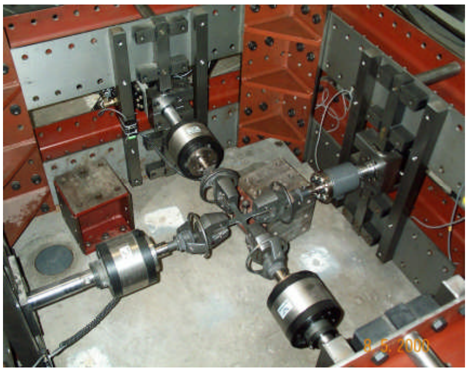

Fig. 1 Biaxial test bench developed at the VUB

4. Design of the cruciform test specimen

Traditionally, a successful biaxial strength test with cruciform specimens required the following conditions: (i) maximization of the region of uniform biaxial strain, (ii) minimization of the shear strains in the biaxially loaded test zone, (iii) minimization of the strain concentrations outside the test zone, (iv) specimen failure in the bi-axially loaded test zone and (v) repeatable results [3,8,10,11,12]. It has been proven extremely difficult to develop cruciform specimens that simultaneously fulfil all these requirements. Conditions (i) and (ii) were required if strains were measured at the centre of the specimen with a strain gage or extensometer where one average strain value was obtained over their length. This average value should be representative for the whole length of the strain gage or extensometer. Thanks to the development of full field methods for strain determination, non-uniformities in strain and occurring shear strains can be quantified getting round these requirements. The strain symmetry condition however remains to be fulfilled and the strains should at least be constant over the length of the strain gage and the subset size of the digital image correlation software, since an average value is given over that size. Conditions (iii) and (iv) are required if reliable strength data under biaxial loading are needed, avoiding failure in the arms or at the corner fillet of the cruciform specimen. These conditions will be checked by comparing the failure strains obtained on standard beamlike specimens with failure strains on uniaxially loaded cruciform specimens measured at the centre of the specimen. For a suitable cruciform geometry, the failure strain values should be equal indicating no early failure occurred elsewhere in the cruciform specimen.

To investigate the influence of parameters like (i) the radius of the corner fillet at the intersection of the arms, (ii) the thickness of the bi-axially loaded test zone in relation to the thickness of the uniaxially loaded arms and (iii) the geometry of the bi-axially loaded test zone, orthotropic finite element simulations were carried out, allowing a selection of final candidate geometries to be tested experimentally. Afterwards, the numerical results were compared with experimental ones using the digital image correlation technique for full field strain measurements.

The finite element simulations were performed with the commercial software *Ansys* using element type *plane 42*, which is used here as a plane stress element. It is defined by four nodes having two degrees of freedom at each node: translations in the nodal x and y directions. The element coordinate system was parallel to the global coordinate system. The material modelled was glass fibre reinforced epoxy with a $[(\pm 45/0)_4/\pm 45]_T$ lay-up. The material system and stacking sequence are typical of wind turbine rotor blade construction. Cruciform specimens were machined from plates produced by LM Glasfiber, Denmark, using RTM (resin transfer moulding) technology. When cured, the [±45] plies have a thickness of 0.61 mm and the [0] ones of 0.88 mm. This gives a total thickness of 6.57 mm for the laminate of the cruciform specimen and of 3.59 mm where one group of [±45/0] was milled away at each side of the specimen. Homogenized elastic properties for the composite laminate, derived by means of Classical Lamination Theory, were used for the simulations. The load ratio between the x- and y-directions was chosen equal to the respective strength ratio of the laminate, F_x/F_y = 46.2 kN/12 kN. The width of the arms is 25 mm; the total length of the specimen is 250 mm. In Fig.2, finite element results are shown of the first principal strain for four subsequent geometries while in Fig.3 the occurring shear strain is presented. The bi-axially loaded test zone was zoomed in, but the finite element calculations were performed with the arms included.

A full field experimental technique that enables the assessment of the overall strain distribution in the cruciform specimens is absolutely necessary. Strain measurements using a strain gage or extensometer are not sufficient because both give an average value of the deformation along their gauge length. To be able to study the symmetry of the strains and the occurring shear strains experimentally, a full field strain method is necessary.

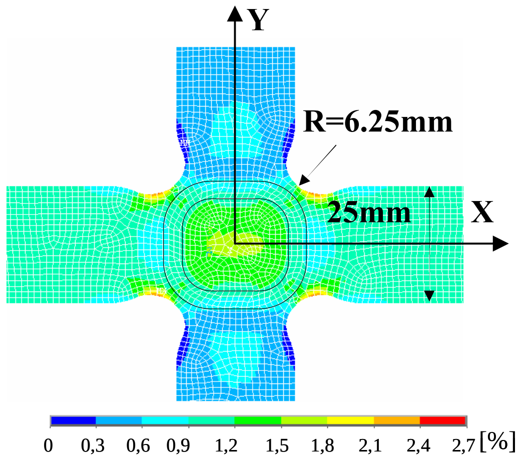

Fig.2. Finite element results of the first principal strain for four cruciform geometries.

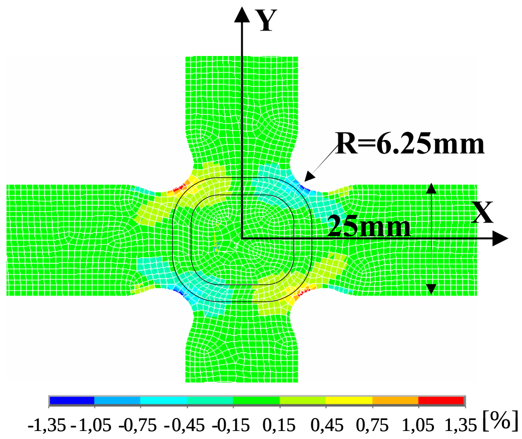

Fig.3. Shear strain distributions for four cruciform geometries.

Digital image correlation (DIC) is an experimental technique, which offers the possibility to determine displacement and deformation fields at the surface of objects under any kind of loading, based on a comparison between images taken at different load steps. The software processes and visualizes the data gathered in order to obtain an impression of the distribution of strains in the measured object. A measurement session consists of taking several pictures of the object of interest with a Charge Coupled Device (CCD) camera. In this case, see Fig.4, two cameras were used to be able to measure both in-plane and out of plane displacements on specimens not entirely flat as is the case for the specimens with a milled surface in the centre. Each picture corresponds to a different loading step. The camera uses a small rectangular piece of silicon, which has been segmented into an array of 1392 by 1040 individual light-sensitive cells, also known as photo sites or pixels. Every pixel stores a certain grey scale value ranging from 0 to 255, in agreement with the intensity of the light reflected by the surface of the tested specimen.

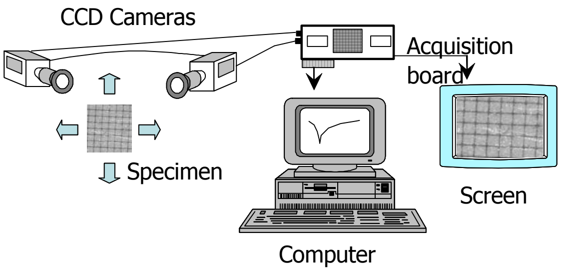

Fig. 4 Digital Image Correlation system

The same cruciform geometries as studied in the finite element simulations were tested experimentally. Results for the first principal strain are shown in Fig.5. Similar distribution of the strain is obtained as in the finite element simulations. Only in the transition zone between the intact laminate and the milled area, high strains are observed with the digital image correlation technique but not in the finite element simulations. This is due to the fact that the milling requires more detailed finite element models to simulate the decrease in number of layers gradually.

Shear strain distributions for the four tested geometries are presented in Fig. 6. The results are similar as the finite element simulations with zero shear stains in the uniaxially loaded arms and in the centre of the specimen and shear strains at the corner fillets.

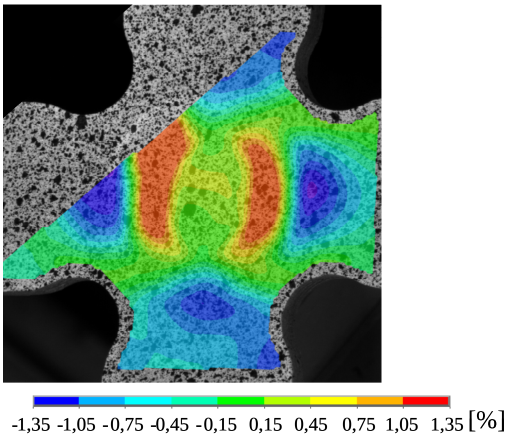

Fig.5. Digital image correlation results of the first principal strain of the selected geometry.

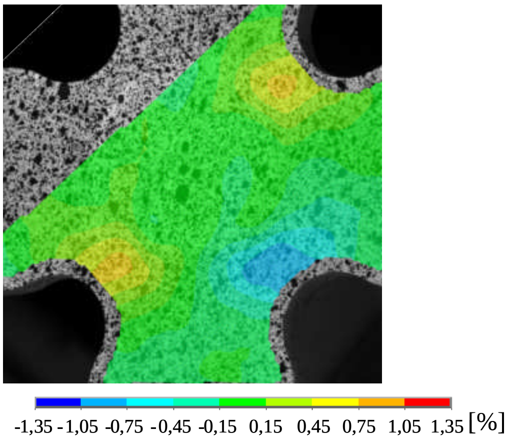

Fig. 6. Digital image correlation results of the shear strains of the selected cruciform geometry.

In figure 7 the experimental biaxial test results are given for different loading ratio's.

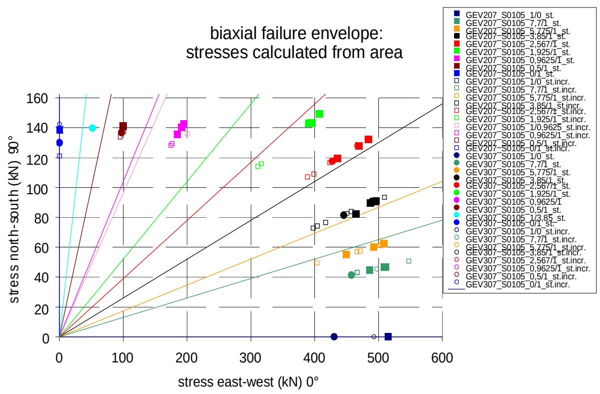

Fig. 7. Biaxial test results for different load ratio's

Pictures recorded immediately prior to (upper frame) and during failure (lower frame) are shown in Fig.8

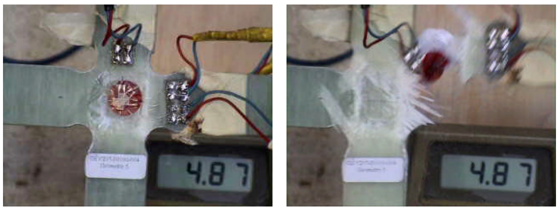

48.7kN failure, 48.7kN

Fig. 8 Pictures of the failure modes

5. Inverse method

5.1 Introduction

For uniaxial testing the conversion from force to stress is straightforward because the cross section is known and consequently stiffness data can be easily calculated. In order to define stiffness data using biaxial loaded cruciform test specimen an alternative mixed numerical experimental technique belonging to the category of inverse problems was developed. The method developed at the Royal Military Academy (RMA), which integrates an optimization technique, a full-field measurement technique and a finite element method [13,14]. In this paper, a method is proposed for the identification of the in-plane engineering constants E_1, E_2, G_{12} and ν_{12} of an orthotropic material based on surface measurements. The responses of the system, i.e. the surface displacements are measured with digital image correlation. Strains are subsequently calculated, based on the measured displacement field. A finite element model of the cruciform specimen serves as numerical counterpart for the experimental set-up. The difference between the experimental and numerical strains (the cost function) is minimized in a least squares sense by updating the values of the engineering constants. The optimization of the parameters is performed by a Gauss-Newton method.

In contrast to a direct problem which is the classical problem where a given experiment is simulated in order to obtain the stresses and the strains, inverse problems are concerned with the determination of the unknown state of a mechanical system, using information gathered from the response to stimuli on the system [15]. Not only the boundary information is used, but relevant information coming from full-field surface measurements is integrated. The inverse method described here can be narrowed to parameter identification, as the only item of interest is the determination of the constitutive parameters. The values of these parameters cannot be derived immediately from the experiment due to the specimen geometry. A numerical analysis is necessary to simulate the experiment. However, this requires that the material parameters are known. The identification problem can be formulated as an optimization problem where the function to be minimized is an error function that expresses the difference between numerical simulation and experimental results. In the present case the strains are used as output data. (Fig. 9) represents the flow chart of the inverse modeling problem.

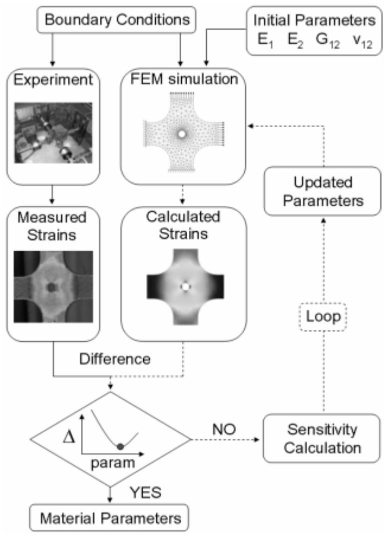

Fig. 9 - Flow-chart of determination process

5.2 Optimization algorithm

The optimization of the apparent engineering constants is performed by a Gauss-Newton method. The cost function that is minimized is a simple least squares formulation. Expression (1) shows the form of the least-squares cost function that is minimized. The residuals in the function are formed by the differences between the experimental and the numerical strains.

$$C(\underline{p}) = C(\underline{\varepsilon}(\underline{p}),\underline{p}) = \sqrt{\sum_{i=1}^{n}\left\langle \frac{\varepsilon_i^{num}(\underline{p}) - \varepsilon_i^{exp}}{\varepsilon_i^{exp}} \right\rangle^2} \qquad (1)$$

The necessary condition for a cost function to attain its minimum is expressed by equation (2). The partial derivative of the function with respect to the different material parameters has to be zero. By developing a Taylor expansion of the numerical finite element strains around a given parameter set, an expression is obtained in which the difference between the present parameters and their new estimates is given (3).

$$\frac{\partial C(\underline{p})}{\partial p_i} = \frac{1}{C(\underline{p})} \sum_{j=1}^{n} \left(\frac{\varepsilon_i^{num}(\underline{p}) - \varepsilon_i^{exp}}{\varepsilon_i^{exp}} \right) \frac{\partial \varepsilon_j^{num}}{\partial p_i} = 0 \tag{2}$$

$$\varepsilon_i^{num}(\underline{p}) \cong \varepsilon_i^{num}(\underline{p}^k) + \sum_{j=1}^{m} \frac{\partial \varepsilon_i^{num}(\underline{p}^k)}{\partial p_j} \left(p_j - p_j^k \right) \tag{3}$$

When substituting this last expression into expression (2) and after rearranging some terms, expression (4) yielding the parameter updates is obtained.

$$\underline{\Delta p} = \left(\underline{\underline{S}}^t \underline{\underline{S}} \right)^{-1} \underline{\underline{S}}^t \left(\varepsilon^{exp} - \varepsilon^{num}\left(\underline{p}^k \right) \right) \tag{4}$$

in which the following elements are:

$\underline{\Delta p}$: column vector of the parameter updates of E_1, E_2, G_{12} and v_{12}

$\underline{\varepsilon}^{exp}$: column vector of the experimental strains

$\underline{\varepsilon}^{num}(\underline{p}^k)$: column vector of the finite element trains as a function of the parameters at iteration k

$\underline{p}^k$: the four parameters at iteration step k

$\underline{\underline{S}}$: sensitivity matrix

5.3 Sensitivity calculation

The sensitivity matrix (5) groups the sensitivity coefficients of the strain components in every element of the finite element mesh with respect to the elastic material parameters. The index n in equation (5) stands for the total number of elements. The components of this sensitivity matrix can be derived analytically from the constitutive relation between stress and strain, which is given by expression (6) in the case of a plane stress problem.

The stresses that are used in the calculation of the derivatives are taken from the converged simulation in the actual iteration step. The values of the parameters are taken from the previous iteration step.

$$\underline{\underline{S}} = \begin{bmatrix} \frac{\partial \varepsilon_x^1}{\partial E_1} & \frac{\partial \varepsilon_x^1}{\partial E_2} & \frac{\partial \varepsilon_x^1}{\partial G_{12}} & \frac{\partial \varepsilon_x^1}{\partial \nu_{12}} \\ \frac{\partial \varepsilon_y^1}{\partial E_1} & \frac{\partial \varepsilon_y^1}{\partial E_2} & \frac{\partial \varepsilon_y^1}{\partial G_{12}} & \frac{\partial \varepsilon_y^1}{\partial \nu_{12}} \\ \frac{\partial \gamma_{xy}^1}{\partial E_1} & \frac{\partial \gamma_{xy}^1}{\partial E_2} & \frac{\partial \gamma_{xy}^1}{\partial G_{12}} & \frac{\partial \gamma_{xy}^1}{\partial \nu_{12}} \\ \vdots & \vdots & \vdots & \vdots \\ \frac{\partial \varepsilon_x^n}{\partial E_1} & \frac{\partial \varepsilon_x^n}{\partial E_2} & \frac{\partial \varepsilon_x^n}{\partial G_{12}} & \frac{\partial \varepsilon_x^n}{\partial \nu_{12}} \\ \frac{\partial \varepsilon_y^n}{\partial E_1} & \frac{\partial \varepsilon_y^n}{\partial E_2} & \frac{\partial \varepsilon_y^n}{\partial G_{12}} & \frac{\partial \varepsilon_y^n}{\partial \nu_{12}} \\ \frac{\partial \gamma_{xy}^n}{\partial E_1} & \frac{\partial \gamma_{xy}^n}{\partial E_2} & \frac{\partial \gamma_{xy}^n}{\partial G_{12}} & \frac{\partial \gamma_{xy}^n}{\partial \nu_{12}} \end{bmatrix} \tag{5}$$

$$\begin{Bmatrix} \varepsilon_x \\ \varepsilon_y \\ \gamma_{xy} \end{Bmatrix} = \begin{bmatrix} \frac{1}{E_1} & -\frac{v_{12}}{E_1} & 0 \\ -\frac{v_{12}}{E_1} & \frac{1}{E_2} & 0 \\ 0 & 0 & \frac{1}{G_{12}} \end{bmatrix} \begin{Bmatrix} \sigma_x \\ \sigma_y \\ \tau_{xy} \end{Bmatrix} \tag{6}$$

5.4 Experimental results

5.4.1 Tests on rectangular specimen

An extended database of experimental static and fatigue results on beamlike glass fibre reinforced epoxy specimens with a $[(+45° \ -45° \ 0°)_3(+45°\text{-}45°)]$-lay-up has been set-up within the framework of the Optimat Blades project [16]. For the glass fibre reinforced composite laminate with the mentioned lay-up the average and standard deviation material parameter results of about four hundred traditional beamlike tests are given in (Tabel 1). No information about the shear modulus is available for this lay-up. Only for a single unidirectional ply, information exists from off-axis tests and tests on a (+45°/-45°) lay-up given in (Tabel2). Based on the ply data, the theoretically expected properties of the laminate can be calculated using classical laminate theory (Tabel 3).

Table 1. Material properties of the laminate obtained on beamlike specimens

	E_1 GPa	E_2 GPa	G_{12} GPa	v_{12} -
average	27.03	14.21	-	0.455
standard deviation	1.19	0.85	-	0.042

Tabel 2. Material properties of the ply used in the laminate obtained on beamlike specimens

	E_1 GPa	E_2 GPa	G_{12} GPa	ν_{12} -
average	39.10	14.44	5.39	0.294
standard deviation	2.10	0.98	1.77	0.027

Tabel 3. Calculated material properties of the laminate using classical laminate theory (the apparent engineering constants of the laminate)

	E_1 GPa	E_2 GPa	G_{12} GPa	ν_{12} -
average	28.48	16.27	8.33	0.407

5.4.2 Tests on cruciform specimen (engineering constants)

For the identification of the four independent elastic orthotropic parameters, a perforated and a non-perforated specimen are used. The reason of testing a specimen with a hole is the aim to influence the overall deformation field and to make the measured strain fields more sensitive to the different material parameters. Because we are dealing with an experimentally obtained strain field, this can be important. The specimens are subjected to three different ratios of biaxial tensile loads : 2.56/1, 3.85/1 and 5.77/1. Five successive load steps are imposed per ratio, so this means that fifteen independently measured strain field triplets are available per specimen for the identification process. The same loads are used in the finite element simulation. A plane stress model is used with a uniformly distributed load as boundary condition. The convergence criterion used in the optimization phase ends the iteration process when the relative value of the parameter updates is inferior to 0.01%. In all of the optimization runs, the convergence criterion is reached in less than 13 iterations.

The results of the identification process are shown in (Table 4) and (Table 5) for both perforated and non-perforated specimen, in terms of the mean parameter value and its corresponding standard deviation. They are obtained based on the fifteen imposed load steps considered per specimen. The starting values for each of the parameters are mentioned as well.

It can be observed that the difference between the results for both specimen types is reasonably small. The stability of the results obtained with the non-perforated specimen is slightly larger. This is probably due to the fact that the strain field is less complex and therefore easier to measure with the digital image correlation technique than in the case of the perforated specimen.

Table 4. Material properties of perforated cruciform specimen

	E_1 GPa	E_2 GPa	G_{12} GPa	ν_{12} -
starting values	15	10	10	0.3
average	25.11	12.17	7.05	0.483
standard deviation (%)	5.4	6.8	8.9	7.7

Table 5. Material properties of non-perforated cruciform specimen

	E_1 GPa	E_2 GPa	G_{12} GPa	ν_{12} -
starting values	15	10	10	0.3
average	25.11	13.31	7.69	0.467
standard deviation (%)	2.8	6	6.8	6.6

6. Conclusions

The combination of finite element simulations and experiments performed on different cruciform geometry types using the digital image correlation technique for full field strain measurements, led to the selection of a suitable geometry for biaxial testing of fibre reinforced composite laminates. This geometry has a reduced thickness in the central region of the specimen, in combination with a fillet corner between two arms inside the material. These features cause failure to occur in the bi-axially loaded test zone, rather than in the uni-axially loaded arms giving failure strains comparable to strains obtained on beamlike specimens for the uniaxial load ratios. The digital image correlation technique used for full field strain measurements offers significant advantages over conventional techniques such as strain gauges. The spatially resolved strains led to a better understanding of the behaviour of composites under bi-axial loads. The strain values obtained with the digital image correlation technique are comparable with those calculated in the finite element simulations. Using the proposed geometry strength data was obtained for different load ratio's.
An inverse method has been proposed to determine the elastic parameters (E1, E2, G12 and v12) of a glass fibre reinforced epoxy with a [(+45° -45° 0°)3(+45°-45°)]-lay-up. Two specimen geometries are used: a regular cruciform specimen and a cruciform specimen into whom a central hole is drilled. The latter is made in order to enhance the already heterogeneous deformation field. The

method is based on a finite element calculated strain field of a cruciform specimen loaded in both orthogonal axes and the measured strain field obtained by digital image correlation. The obtained material parameters agree reasonably well with the values obtained by traditional uni-axial tensile tests. However, the results based on the regular cruciform specimen without hole, show less variance than the results obtained with the perforated specimen. This is possibly due to the fact that the digital image correlation technique has some difficulties measuring steep deformation gradients, hence inducing errors in the measurement of the displacement and strain maps. Further investigation is needed to clarify this inconvenience. The objective of the experiment is to enforce a material behaviour that exposes the different elastic material parameters. If this is achieved by a non-perforated specimen, there is no need for a more complex geometry which will possibly lead to more measurement errors.

7. Acknowledgements

This project is supported by the Belgian Science Policy through the IAP P05/08 project and the European Commission in the framework of the specific research and technology development program Energy, Environment and Sustainable Development with contract number ENK6-CT-2001-00552. The authors also express their gratitude to Hans Tommerup Knudsen from LM-Glassfiber in Denmark for his effort in producing the cruciform specimens.

8. References

[1] Lin WP, Hu HT, Parametric study of failure stresses in fibre reinforced composite laminates subjected to biaxial tensile load, *Journal of Composite Matererials*, vol 36 (12), 1481-1504, 2002

[2] Boehler JP, Demmerle S, Koss S, A new direct biaxial testing machine for anisotropic materials, *Experimental Mechanics*, vol 34 (1), 1-9, 1994

[3] Soden PD, Hinton MJ, Kaddour AS, Biaxial test results for strength and deformation of a range of E-glass and carbon fibre reinforced composite laminates : failure exercise benchmark data, *Composites Science and Technology*, vol 62 (12), 1489-1514, 2002

[4] Welsh JS, Adams DF. Development of an electromechanical triaxial test facility for composite materials. Exp Mech 2000; 40(3): 312-320.

[5] Zouani A, Bui-Quoc T, Bernard M, A proposed device for biaxial tensile fatigue testing, *Fatigue and Fracture*, ASME PVP-323, vol 1, 331-339, 1996

[6] Swanson SR, Christoforou AP, Colvin GE, Biaxial testing of fiber composites using tubular specimens, *Experimental Mechanics*, vol 28 (3), 238-243, 1988

[7] Pascoe KJ, de Villers JWR, Low cycle fatigue of steels under biaxial straining, *Journal of Strain Analysis*, vol 2 (2), 117-126, 1967

[8] Parsons MW, Pascoe KJ, Development of a biaxial Fatigue testing rig, *Journal of Strain Analysis*, vol 10, 1-9, 1975

[9] Smits A, Van Hemelrijck D, Philippidis TP, Cardon A, Design of a cruciform specimen for biaxial testing of fibre reinforced composite laminates, *Composites Science and Technology*, vol 66 (7-8), 964-975, 2006

[10] Yu Y, Wan M, Wu XD, Zhou XB. Design of a cruciform biaxial tensile specimen for limit strain analysis by FEM. Journal of Materials Processing Technology 2002; 123(1): 67-70.

[11] Mayes JS, Welsh JS, Key CT. Biaxial failure envelope for a glass fabric reinforced composite laminate. Final Report PO N00167-01-M-0246 Mayes Consulting Engineers. 2002. p. 1-13.

[12] Welsh JS, Adams DF. An experimental investigation of the biaxial strength of IM6/3501-6 carbon/epoxy cross ply laminates using cruciform specimens. Compos Part A- Appl S 2002; 33(6): 829-839.

[13] Lecompte D, Smits A, Sol H, Vantomme J, Van Hemelrijck D, Mixed Numerical-Experimental technique for orthotropic parameter identification using biaxial tensile tests on cruciform specimens, *International Journal of Solids and Structures*, vol 44 (5), 1628-1642, 2007

[14] Lecompte D, Elastic and elasto-plastic material parameter identification by inverse modeling of static tests using digital im age correlation, PhD Thesis, Free University of Brussels (VUB), 1-220, 2007

[15] Bui HD, Inverse problems in the Mechanics of Materials : An introduction, *CRC Press Inc. Florida*, 1-224, 1994

[16] Reliable optimal use of materials for wind turbine rotor blades, *Optimat Blades*, contract n° ENK6-CT-2001-00552, project n° NNE5-2001-00174